

AD-A051 302

NAVAL RESEARCH LAB WASHINGTON D C
ABSORPTION OF LASER LIGHT IN LASER FUSION PLASMAS. (U)
DEC 77 B H RIPIN

F/0 18/1

UNCLASSIFIED

NRL-MR-3684

SBIE-AD-E000 118

NL

| OF |
AD
A051 302



AD A 051 302

ade000118
NRL Memorandum Report 3684

Absorption of Laser Light in Laser Fusion Plasmas

B. H. RIPIN

*Laser Plasma Branch
Plasma Physics Division*

12

AD No. _____
DDC FILE COPY

December 1977



DDC
RECEIVED
MAR 16 1978
B

NAVAL RESEARCH LABORATORY
Washington, D.C.

Approved for public release; distribution unlimited.

REPORT DOCUMENTATION PAGE		READ INSTRUCTIONS BEFORE COMPLETING FORM
1. REPORT NUMBER NRL Memorandum Report 3684 ✓	2. GOVT ACCESSION NO.	3. RECIPIENT'S CATALOG NUMBER
6. TITLE (and Subtitle) ABSORPTION OF LASER LIGHT IN LASER FUSION PLASMAS,		9. TYPE OF REPORT & PERIOD COVERED Interim report on a continuing NRL problem.
7. AUTHOR(s) B.H. Ripin		8. CONTRACT OR GRANT NUMBER(s)
9. PERFORMING ORGANIZATION NAME AND ADDRESS Naval Research Laboratory ✓ Washington, D.C. 20375		10. PROGRAM ELEMENT, PROJECT, TASK AREA & WORK UNIT NUMBERS NRL Problem H02-29A
11. CONTROLLING OFFICE NAME AND ADDRESS Department of Energy Washington, D.C. 20545		12. REPORT DATE December 1977
		13. NUMBER OF PAGES 34
14. MONITORING AGENCY NAME & ADDRESS (if different from Controlling Office) 12 34p.		15. SECURITY CLASS. (of this report) UNCLASSIFIED
16. DISTRIBUTION STATEMENT (of this Report) Approved for public release; distribution unlimited 14 NRL-MR-3684		15a. DECLASSIFICATION/DOWNGRADING SCHEDULE
17. DISTRIBUTION STATEMENT (of the abstract entered in Block 20, if different from Report) 18 SBIE 19 AD-E000 118		DDC RECEIVED MAR 16 1978 REGULATIVE B
18. SUPPLEMENTARY NOTES Work performed at the Naval Research Laboratory under the auspices of the Department of Energy. This paper was first presented as an invited paper at the 1977 American Physical Society - Plasma Physics Division Meeting, Atlanta, Georgia, 8 November 1977.		
19. KEY WORDS (Continue on reverse side if necessary and identify by block number) Backscatter Brillouin Reflection Backreflection Absorption Instability Plasma Laser fusion 10% + the 15th power to 10% to the 16th power 59 cm		
20. ABSTRACT (Continue on reverse side if necessary and identify by block number) Variables affecting the absorption of high-irradiance (10^{15} - 10^{16} W/cm ²) laser light in plasmas were studied experimentally and where possible related to theory. It was found that temporally structured laser pulses, simulating those required in many pellet implosion designs, exhibit very enhanced backscatter consistent with Brillouin. The variation of absorption with focal position and incident irradiance, and the critical surface structure inferred from scattered laser light will be described and their implications to laser fusion discussed.		

251 950

LB

Preceding Page BLANK - NOT FILMED

ABSORPTION OF LASER LIGHT IN LASER FUSION PLASMAS

There are many factors which affect the absorption of high-irradiance laser light in plasmas. The subject of this paper will be to address some of these factors investigated in experiments at NRL. It is found, for example, that the transition from high irradiance single pulse irradiation to a structured pulse may be accompanied by profound changes in the physics.

In Figure 1 we indicate how laser fusion physics may be divided into three almost distinct elements. First, the light is absorbed. The obvious questions are; how much?; how?; where?; and by what mechanisms it is absorbed? Then the absorbed energy is transported both inward to the ablation surface and outward into the expansion plasma. Third, the plasma reacts hydrodynamically and bulk motion of the plasma results. All three elements are, of course, related and affect each other. For example, both heat transport and hydrodynamic motion change the temperature and density scale lengths in the absorption region and may thereby change the absorption process. I will point out a striking example of this later on. Finally the interaction physics depends upon what pulse shape or duration that is used. Up to the present most experiments have been performed with single-short-high-irradiance pulses due to energy limitations of existing lasers. However, realistic pulse shapes proposed for laser fusion, such as originally proposed by J. Nuckolls¹, are usually longer and are often highly shaped. We will see later that the physics of the interaction is altered considerably with structured pulses.

The parameters of these experiments as well as the major variations made for these absorption studies are listed in Table I. We use one beam of the Pharos II Nd-laser ($\lambda = 1.06 \mu\text{m}$) focused onto planar targets with an f/1.9 lens. Polished polystyrene CH targets are irradiated in the range of 10^{15} - 10^{16} W/cm² with 75 psec pulses. Sometimes polished Al targets are used to check atomic number (Z) dependency. The experimental setup is shown in Fig. 2. Within the evacuated target chamber are several diagnostics, including, an array of (18) scattered light calorimeters, an electron spectrometer (30-1000 keV), a harmonic emission PIN-diode ($n = 1-5$), charge collectors and a set of 15 x-ray continuum detectors which cover the range of 1-300 keV. In addition a spectrometer monitored harmonic emission, a Raman shifted probe light (6329 Å, 35 psec) was used to obtain interferograms of the underdense plasma at varying times in its

Note: Manuscript submitted December 30, 1977.

White Section	<input checked="" type="checkbox"/>
Buff Section	<input type="checkbox"/>
ABILITY CODES	
Disc.	and/or SPECIAL
A	

development. Of course, the incident, backreflected and transmitted light were monitored with calorimeters. Two important laser beam monitors, used on each shot, are also indicated. First, the focal shift monitor determines the beam collimation and allows focal position corrections to be made on each shot. Second, a most important diagnostic is the prepulse monitor which indicates the presence of any prepulse energy above 10^{-8} of the switched out pulse. The oscilloscope trace of the prepulse monitor on an actual shot, seen in Fig. 2, shows the rejected pulses from the oscillator pulse train at the $0.3 \mu\text{J}$ level before the trace disappears due to the main pulse. A contrast ratio of better than 10^7 is achieved. A photograph of the scattered light calorimeter array is shown in Fig. 3. Two rings, mounted on gimbals, hold the calorimeters in the polarization planes containing the electric vector of the incident beam and the plane perpendicular to this. These calorimeters are calibrated to about 10% precision. Also shown in the photograph are the focusing lens on the right, the transmitted light pickup lens on the left, the target in the middle and the snoot, which is looking down from the top, containing four of the hardest x-ray channels.

The first variation that we will show affects the absorption of laser light in the 10^{15} - 10^{16} W/cm^2 range is whether or not the laser beam is focused onto the target surface. This parameter variation was suggested² as an explanation for total fractional absorption differences reported by several laboratories.³ Garching first verified that this variation did indeed affect absorption.⁴ We have repeated these experiments and in Fig. 4 show the scattered light variations caused by moving the lens through focus. One sees that as one goes out-of-focus in either direction, the backreflection increases and the large angle scattering decreases. Here 0° refers to direct backscatter. The net result, however, after integrating over all 2π -steradians is that in-focus the absorption fraction is about 45% - 50% and out-of-focus the absorption decreases by about 20% , i.e., to 35% - 40% . The plus sign (+) indicates shots taken on aluminum targets and all the other points are on CH targets indicating independence of absorption upon Z.

It is tempting to ascribe the decrease in absorption as due to the decrease in irradiance at the target surface when out-of-focus. The focal spot isointensity contours (separated by $3\times$ from spot-to-spot) obtained by the thin film ablation technique, shown in Fig. 5, indicate that when the target is out-of-focus the irradiance is indeed lowered on the average. However, the peak-to-valley excursions out-of-focus are quite wild and it is difficult to ascribe a meaningful irradiance value as one can do when in-focus.

The absorption dependence upon irradiance variation is tested in a systematic and direct way in Fig. 6. Here again (+) refers to the use of an Al target and the others symbols refer to a CH target taken at the indicated angle from direct backscatter. The beam energy, and hence irradiance, was varied by a factor of 40 between 2.5×10^{14}

and 10^{18} W/cm², approximately the same range that we went through in the focal position study. This was accomplished by keeping the target in focus, pumping the laser at a constant level and placing attenuators in front of the focusing lens. The focal distribution, size, etc. thereby remain constant and only the irradiance is varied. No significant change in absorption is observed over this entire irradiance range.

The conclusion from these studies (Table II) is that laser light absorption is best when the target surface is near focus and, at least within the range of 2.5×10^{14} W/cm² to 10^{18} W/cm², the absorption is insensitive to irradiance.⁵ It is still not clear what causes the absorption change with focal position. It is noted that there are several fundamental differences in the EM field configuration near the target surface in- and out-of-focus. For example; irradiation spot diameter, EM field axial transverse correlation lengths, gradient lengths, etc. all vary with focal position.

The remainder of this paper deals with the differences found between target irradiation with short-single-pulses and structured laser pulses such as illustrated in Fig. 7. Since laser fusion schemes usually require longer and more structured pulses than are presently used, we attempt to simulate a structured pulse with a prepulse and a subsequent high-irradiance main pulse. The prepulse forms a target plasma (much as the long low-irradiance foot of a structured pulse would) and the main pulse simulates the high irradiance spike at the end of a structured pulse. We find a striking change in the absorption and, possibly, heat transport with such structured pulses.

Precisely controlled prepulses are introduced into the beam by the beam splitter - dog leg arrangement shown in Fig. 8a placed after the laser oscillator. The temporal separation between the prepulse and main pulse has been set at 2 nsec and the relative amplitudes are adjusted with attenuators A_p and A_m . As before the target is planar CH placed normal to the laser (unless noted otherwise) in the focus of an f/1.9 lens. Backreflection is monitored with a calorimeter and the angular distribution of scattered light outside the lens is monitored with the array of 18 mini-calorimeters as shown in Fig. 8b.

We have plotted in Fig. 9 some very striking results from these experiments as a function of prepulse energy/total incident energy (η).⁶ The backreflection fraction of the main pulse increases dramatically with the prepulse level. Without any prepulse the backreflection into our f/1.9 lens is $16 \pm 2\%$. With the addition of a prepulse, even at the 10^{-4} level, an increase in backreflection occurs. With large prepulses, the main pulse backreflection is almost triple that of the single-pulse case. The total absorption fraction decreases from 45-50% when single pulses are used to about 30% when large prepulses are employed. Therefore, a large increase in backscatter and a reduction in absorption results when a structured pulse is used instead of

a single pulse. This change in absorption is not due to a focal position shift. On some shots (*) the target was moved such that the main pulse was focused onto the prepulse formed plasma instead of the target surface with little change of results.

The variation of backscatter with incident irradiance is shown in Fig. 10. At a fixed prepulse fraction the main pulse backreflection is seen to linearly increase with incident energy (or irradiance) in the 10^{15} - 10^{16} W/cm² range. No evidence of saturation is seen within this range! In Fig. 10 the open circles are shots taken with the CH target normal to the laser beam axis and the closed circles are shots taken with the target rotated by 45° . The dashed line shows the decrease of backreflection, obtained from Fig. 9, due to the reduction of the prepulse energy alone. The significant increase in backreflection and the lack of saturation with increasing irradiance suggests that a backscatter instability is responsible.

The most obvious potentially responsible instability that comes to mind is the stimulated Brillouin backscatter instability.⁷ The basic mechanisms driving this instability are indicated in Fig. 11. The Brillouin instability is a three-wave process in which the incident EM wave beats with a reflected EM wave somewhere in the underdense plasma. The resulting partial standing wave pattern drives up an ion wave with half the incident wavelength. This ion wave has the correct periodicity to directly backscatter more energy--thereby increasing the ion wave amplitude further. The whole process is therefore unstable. This instability has the properties listed in Table III, which we will now test for.

The threshold for the Brillouin instability is in the irradiance region of 10^{13} W/cm² for most reasonable density gradients in the underdense plasma. This was shown experimentally by us in 1974 when the first time-resolved backscatter spectra were obtained of the Brillouin instability.⁸ The density scale lengths in the plasma produced by the prepulse at the time of arrival of the main pulse are long enough ~ 100 μ m for high level Brillouin growth. Figure 12 shows an interferogram, axial density profile and Abel inverted density distribution for the plasma at the time of arrival of the main pulse when a 20% ($\eta = 0.2$) prepulse is employed. Note that the equidensity contours (light lines) are becoming relatively flat and parallel to the target surface for densities above 4% of critical, i.e. for $n > .04 n_c$. At lower densities an on-axis density depression is evident.

Now a very crucial question is: Where in the underdense plasma does the enhanced reflection process occur? To answer this question we rotate the target by an angle θ as indicated in Fig. 13. If the turning point density surface is approximately aligned with the target surface then the maximum density, n_t , reached by the incident electromagnetic wave is $n_t = n_c \cos^2 \theta$.⁹ If at some target angle θ

one still has high backreflection then the process must occur for densities $n < n_c$. We will show that the assumption that n_c is indeed fairly well aligned with the target surface is valid, but let's first see the results. Figure 13 shows that, indeed, as the target is rotated to within 8° of grazing incidence the main pulse backreflection remains very high with a prepulse and decreases to a negligible value with no prepulse. These data suggest that the instability occurs in the very underdense ($n < 0.1 n_c$) plasma, subject to the assumption of planar geometry for n_c .

We will use a specular reflection test for the orientation and geometry of the turning point surface. This test is illustrated in Fig. 14. If the surface is planar and aligned with the target surface the specular reflection goes off at the target mirror angle. On the other hand if the turning point surface is curved then the specular reflection will go off at the local plasma mirror angle and will not peak at the target mirror angle. The results of this test are shown in Fig. 15. The target is rotated $67\frac{1}{2}^\circ$ and burnpaper surrounds the target to monitor the specular reflected light from the target. A shielded hole allows the incident beam to enter and be focused onto the target surface. Three cases are shown in Fig. 15. First, single-short-pulse irradiation results in the expected low backreflection ($< 2^\circ$) and specular reflection at the mirror angle of the target (135°).⁹ Second, a small (12°) prepulse is applied the standard 2 nsec ahead of the main pulse resulting in enhanced backreflection (15°) and a strong specular reflection at the target angle (135°). The prepulse energy is not sufficient to cause the exposure of the burnpaper and therefore the turning point surface ($n_c = 0.14 n_c$) is aligned with the target surface. Since the backscatter is still very enhanced the back-reflection process occurs at some density $n < 0.14 n_c$. The third example, that with a larger prepulse indicates the same conclusion as the second case, i.e., backreflection of 28° originating at a density less than 14° of critical. This is a result which is very consistent with the Brillouin process.

Another striking feature of Brillouin backscatter found previously in both molecular systems and in laser-plasma cases (the latter at both Garching¹⁰ and NRL in 1973^{11,8}) is the phenomena of optic ray retracing. We illustrate this effect, and show our experimental arrangement to test for it, in Fig. 16. Consider an incident ray, such as the solid line in Fig. 16, which is focused onto a tilted target. Optical ray retracing occurs if upon back-reflection that ray retraces the incident path as opposed to some other trajectory. To test for this we block half the incident beam with burnpaper and monitor both the energy backreflected through the unblocked half and the exposure on the lens side of the burnpaper. No exposure is seen on the burnpaper due to light coming from the target (above the paper exposure threshold (30 mJ/cm^2))

whereas backreflection through the unblocked lens half was high ($\sim 20\%$) and approximately the fraction expected. Experiments were also done with the opposite half of the lens blocked with the same result. We draw two conclusions from this exercise; (1) Optic ray retracing occurs -- suggestive of a stimulated Brillouin backscatter process, and (2) This test eliminates the existence of most pathologic density shapes which would allow the backreflecting density to be near the critical density and still pass the specular reflection test of Figs. 14 and 15.

Observation of stimulated Brillouin backscatter is not at all new in laser-fusion studies. In the 1973-74 period, several groups reported backreflection characteristics consistent with Brillouin.^{8, 10, 11, 12} For example, Fig. 17 is from a backscatter study⁸ in which we showed, with and without a prepulse, the threshold ($\sim 10^{13}$ W/cm²) and time-resolved onset of Brillouin backscatter (Fig. 17c,d). One can see that, in general the backscatter spectra evolves with time, due to competition with Doppler, parametric or other wavelength shifting processes. A time-integrated spectra is not decipherable without other independent knowledge. The backscattered time-integrated spectra in Fig. 17a, however, did exhibit an increasing red shift as the target was rotated from normal incidence consistent with a Brillouin red shift and reduced Doppler component in the backscatter direction.

In the present set of experiments we have not yet taken time-resolved or time-integrated spectra of the backscatter because of the difficulty of ascribing unique interpretations to them. What we have done, however, is to do experiments with band-pass and blocking filters in front of the backscatter calorimeter. In this manner we can determine the spectral region into which most of the energy is backscattered. Using a Corning No. 7-69 filter, which passes 1.06 μm and blocks the UV, visible and $\lambda > 1.1 \mu\text{m}$, we determined that virtually all the enhanced backscatter energy occupies a spectral region very near 1.06 μm . This eliminates, for example, the Raman backscatter processes which, since it spectrally shifts the backscattered light by the electron plasma frequency, would shift the backscatter spectra to the $1.06 < \lambda < 2 \mu\text{m}$ range depending upon the density. This information is valuable because it insures that the bulk of the energy is Brillouin backscattered. A precise time-integrated or even time-resolved spectra restricted to a small region about 1.06 μm could miss a large fraction of the energy scattered into some other spectral region not monitored.

Backscatter data such as shown in Fig. 18, which consists of NRL data taken over the past few years,¹³ also shows an increased back-reflection fraction for the longest pulse length (250 psec). This observation is similar to recent data at LLL and interpretations of it by Bill Kruer.¹⁴ These data suggest that the Brillouin process may well become more severe in larger and longer systems.

In Table IV we summarize what we feel is quite convincing evidence for the Brillouin backscatter instability occurring with structured pulses. The dangerous thing about the Brillouin instability is that, with the larger targets and longer pulses proposed for laser fusion, it is expected to increase in severity. In fact, our experiments do exhibit a marked decrease in absorption and a lack of saturation of the mechanism within our parameter regime.

As I mentioned before, many other parameters such as x-rays, fast electrons, etc. were also measured during these experiments. We have data which suggests that much of the interaction physics with structured pulses may be considerably different from the single-short-pulse case. With the addition of a prepulse, the scattered light angular distribution, ion blowoff, fast-electron energy distributions, x-ray spectra, harmonic emission all act differently. For example, the x-ray data shown in Fig. 19 (taken by F. Young),¹⁵ which compares the cases of single-high-irradiance pulses to cases with varying prepulse level, suggests that the thermal conductivity of the plasmas may be increased with the addition of a small prepulse. For the single-pulse case as the incident energy (irradiance) is increased, the absolute x-ray emission near 1 keV remains almost constant while the higher energy portion of the spectra increases. This suggests that energy flow in the absorption region is "bottled up" and for increasing incident energy the electron population just heats up more. On the other hand, when a small prepulse is applied the x-ray emission near 1 keV increases (even though the absorption decreases) and the higher energy x-ray emission decreases. This may be interpreted as indicative of increased thermal conductivity in the overdense plasma for the prepulse case allowing increased x-ray bremsstrahlung ($\propto n^2$) from a higher density region. Therefore, a small prepulse, which does not decrease absorption too much, may have the beneficial effect of increasing plasma thermal conductivity.

Another experimental observation is that the critical surface roughness appears reduced with the addition of a prepulse. This is deduced by performing a spectral density analysis, developed at NRL,¹⁶ on the scattered light angular distributions.

In Fig. 20 are listed some of the parameter variations that have been shown to affect the physics of the interaction in the 10^{15} - 10^{18} W/cm² irradiance regime. First, for single-short-pulse experiments defocusing decreases absorption whereas a simple irradiance reduction does not have the equivalent effect. This suggests that the details of the EM field, such as size, longitudinal components, or correlation lengths at the target surface are playing a role. No target atomic number dependence was found in these absorption experiments. These experiments tend to bring many of the world's data on absorption into closer agreement. An angle dependent absorption has been shown by others at Sandia,¹⁷ LLL¹⁸ and some European laboratories¹⁹ which suggests that resonance absorption is responsible for some

fraction of the total absorption. It is not clear, at this point, what fraction is absorbed by this mechanism or to the role that critical surface roughness plays in the absorption process.

Also indicated in Fig. 20 are some of the effects that occur with the addition of a prepulse, i.e., due to a structured pulse. The absorption is markedly reduced, probably due to the Brillouin backscatter instability, without any indication of saturation in the 10^{15} - 10^{16} W/cm² region. The plasma thermal conductivity may increase and the critical surface region appears smoother than in the single pulse high-irradiance case.

It is not clear how severe the backscatter problem will be with more realistic pulse shapes until the appropriate experiments are done. The effectiveness of backscatter suppression schemes such as broad bandwidth laser irradiation and high Z targets are still to be tested. Also, some pellet designs,²⁰ announced subsequent to our Brillouin work, operate at lower irradiances where enhanced backscatter may not be as large a problem.

The major points that I wished to emphasize here, however, is that much is still to be learned in the laser-plasma interaction and that it is dangerous to extrapolate through any change in parameters without performing the relevant experiments. My conclusion might be expressed as the moral: Nothing is as simple as it appears before the start nor as difficult as it appears in the middle.

I wish to thank my colleagues: C. M. Armstrong, S. E. Bodner, R. Decoste, R. H. Lehberg, E. A. McLean, J. M. McMahon, J. A. Stamper, R. R. Whitlock, and F. C. Young for their valuable contributions to this paper.

REFERENCES

1. J. L. Nuckolls, L. Wood, A. Thiessen and G. Zimmerman, Nature (London) 239, 139 (1972).
2. B. H. Ripin, Letter to US ERDA, May 1976; B. H. Ripin, et al., NRL Memo Report No. 3591 (1977).
3. R. A. Haas, et al., Phys. Fluids 20, 322 (1977); N. G. Basov, et al., JEPT Lett. 23, 428 (1976); T. P. Donaldson, et al., Phys. Rev. Lett. 37, 1348 (1976); D. V. Giovanielli, et al., LASL Report No. LAUR-77-1074 (1977).
4. C. G. Van Kessel, J. N. Olsen, P. Sachsemaier, R. Sigel, K. Eidmann, and R. P. Godwin, Garching IPP IV/94 (1976).
5. These results were first presented at the 1977 Anomalous Absorption Conference and the 1977 IEEE Conference on Plasma Science (IEEE, NY, 1977), p. 66. Similar results were presented by R. Perkins, et al., *ibid*; M. Richardson, et al., *ibid*.
6. B. H. Ripin, F. C. Young, J. A. Stamper, C. M. Armstrong, R. Decoste, E. A. McLean, and S. E. Bodner, Phys. Rev. Lett. 39, 611 (1977).
7. S. E. Bodner and J. L. Eddleman, Lawrence Livermore Laboratory Report No. 73378, 1971 (unpublished); C. S. Liu, M. N. Rosenbluth, and R. B. White, Phys. Fluids 17, 1211 (1974); D. W. Forslund, J. M. Kindel, and E. L. Lindman, Phys. Fluids 18, 1017 (1975); W. L. Kruer, E. J. Valeo, and K. G. Estabrook, Phys. Rev. Lett. 35, 1076 (1975).
8. B. H. Ripin, J. M. McMahon, E. A. McLean, W. M. Manheimer, and J. A. Stamper, Phys. Rev. Lett. 33, 634 (1974).
9. B. H. Ripin, Appl. Phys. Lett. 30, 134 (1977).
10. K. Eidmann and R. Sigel, Laser Interaction and Related Plasma Phenomena, Vol. 3, p. 667 (1973), Plenum Press, NY (eds., H. Schwarz and H. Hora).
11. J. A. Stamper, et al., Laser Interaction and Related Plasma Phenomena, Vol. 3, p. 713 (1973), Plenum Press, NY (eds., H. Schwarz and H. Hora).

12. C. Yamanaka, et al., *ibid*, pg. 629; L. M. Goldman, J. Soures, and M. J. Lubin, *Phys. Rev. Lett.* 31, 1184 (1973); A. A. Gorokhov, V. D. Dyatlov, V. B. Ivanov, R. N. Medvedev, and A. D. Starikov, *Pis'ma Zh. Eksp. Teor. Fiz.* 21, 62 (1975) [*JETP Lett.* 21, 28 (1975)].
13. B. H. Ripin, E. A. McLean, and J. A. Stamper, *NRL Memo Report No. 3315* (1976).
14. D. W. Phillion, W. L. Kruer, and V. C. Rupert, *UCRL-79769* (1977).
15. F. C. Young and B. H. Ripin, *Bull. Am. Phys. Soc.* 22, 1112 (1977).
16. B. H. Ripin, et al., *NRL Memo Report No. 7838* (1974); *NRL Memo Report No. 3591* (1977); B. H. Ripin, J. A. Stamper, and E. A. McLean, *Bull. Am. Phys. Soc.* 21, 1083 (1976); B. H. Ripin, et al., *IEEE J. Quant. Elec. QE-13*, No. 9, 34D (1977); J. J. Thomson, W. L. Kruer, A. B. Langdon, C. E. Max, and W. C. Mead, *UCRL-79628* (1977).
17. J. S. Pearlman, J. J. Thomson, and C. E. Max, *Phys. Rev. Lett.* 38, 1397 (1977). J. S. Pearlman and M. K. Matzen, *Phys. Rev. Lett.* 39, 140 (1977).
18. K. R. Manes, V. C. Rupert, J. M. Auerbach, P. Lee and J. E. Swain, *Phys. Rev. Lett.* 39, 281 (1977).
19. J. E. Balmer and J. P. Donaldson, *Phys. Rev. Lett.* 39, 1084 (1977); R. P. Godwin, P. Sachsenmaier and R. Sigel, *Phys. Rev. Lett.* 39, 1198 (1977).
20. J. L. Nuckolls, 11th European Conference on Laser Interaction with Matter, Oxford, England, Sept. 19-23 (1977).

Table I

FACTORS AFFECTING ABSORPTION

PARAMETER RANGE:

Nd - LASER $\lambda = 1.06\mu\text{m}$

**FOCUSED ONTO PLANAR TARGETS (CH, Al) AT 10^{15}
- 10^{16} W/cm², 75 psec, f/2 LENS.**

FACTORS STUDIED:

FOCAL POSITION

IRRADIANCE

STRUCTURED PULSES

Table II

**FOCAL POSITION AND IRRADIANCE
VARIATIONS**

- **BEST ABSORPTION NEAR FOCUS**
- **ABSORPTION INDEPENDENT OF IRRADIANCE**

Table III

PROPERTIES OF BRILLOUIN BACK REFLECTION

- THRESHOLD
- GAIN INCREASES WITH SCALE LENGTH
- BACK-REFLECTION INCREASES WITH IRRADIANCE
- INSENSITIVE TO TARGET ANGLE
- OCCURS IN UNDERDENSE PLASMA
- OPTIC RAYS RETRACE
- SCATTERED ENERGY NEAR $\omega_c - \omega_{ia} \approx \omega_c$

Table IV

EVIDENCE FOR BRILLOUIN BACK REFLECTION

- ✓ ABOVE THRESHOLD
- ✓ BACK REFLECTION INCREASES WITH PREPULSE LEVEL
- ✓ BACKREFLECTION INCREASES WITH IRRADIANCE
- ✓ BACKREFLECTION INSENSITIVE TO TARGET ANGLE
- ✓ BACKREFLECTION OCCURS IN UNDERDENSE PLASMA
- ✓ OPTIC RAYS RETRACE
- ✓ SCATTERED ENERGY NEAR ω_c .
- BRILLOUIN COULD INCREASE WITH LARGER TARGETS AND LONGER PULSES

LASER FUSION PHYSICS

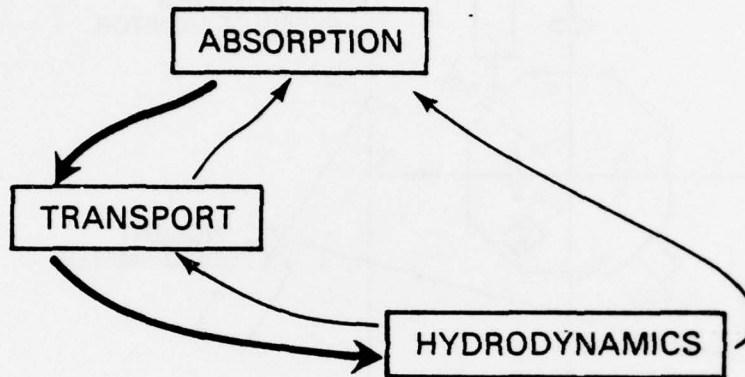


Fig. 1 - Inter-relationship between plasma absorption, heat transport and hydrodynamic plasma motion

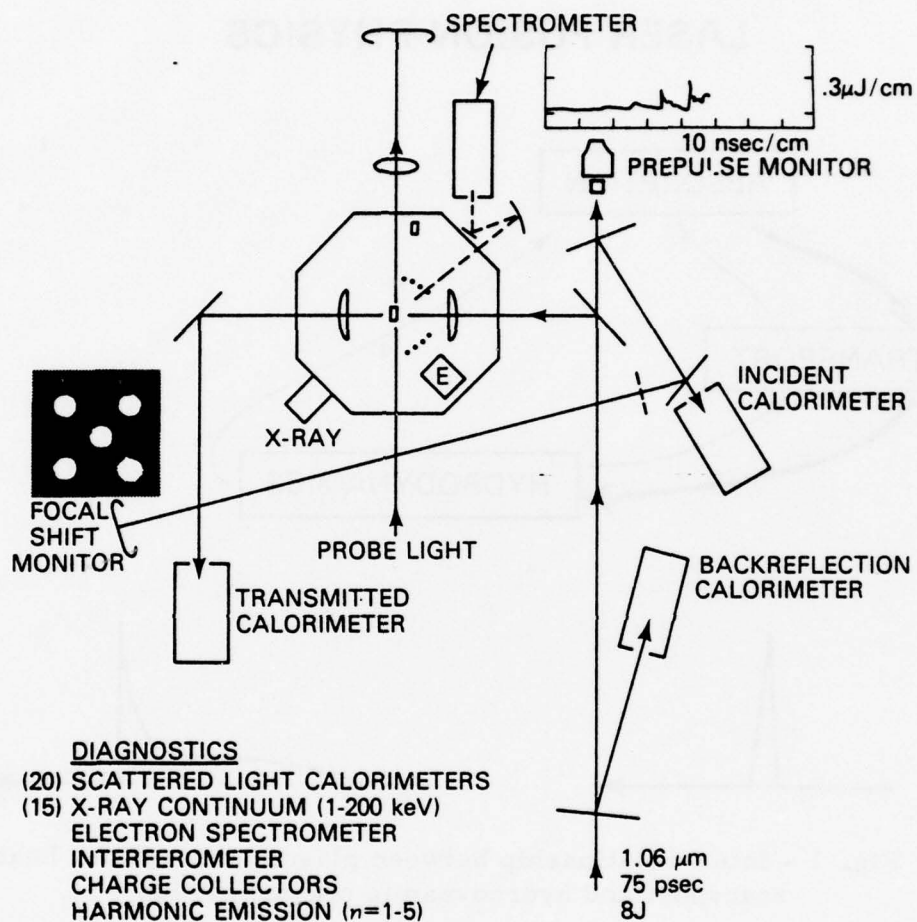


Fig. 2 - Experimental setup for these experiments indicating beam monitors, focusing arrangement and diagnostics

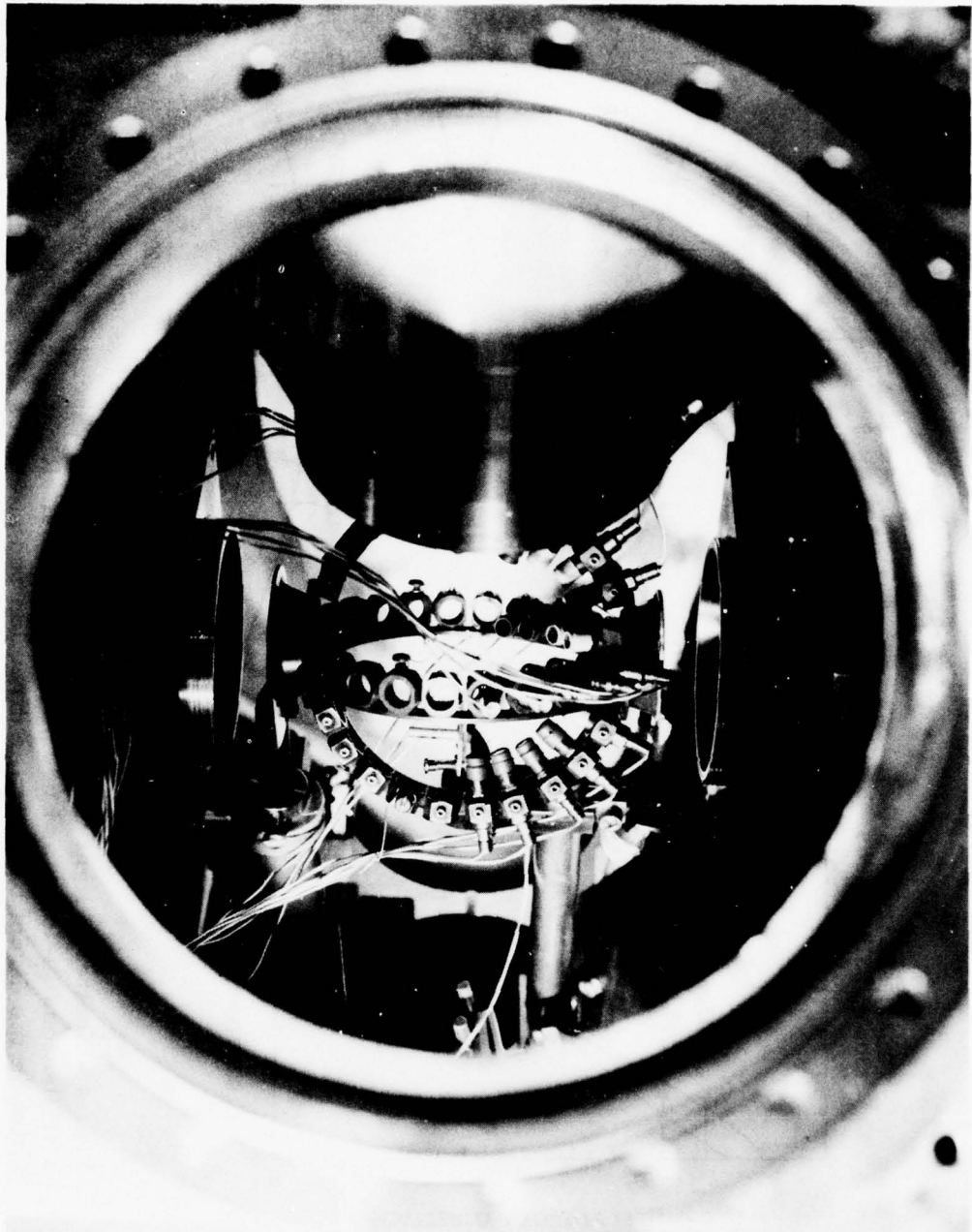


Fig. 3 - Photograph of the mini-calorimeter array used to measure the angular distribution of scattered laser light

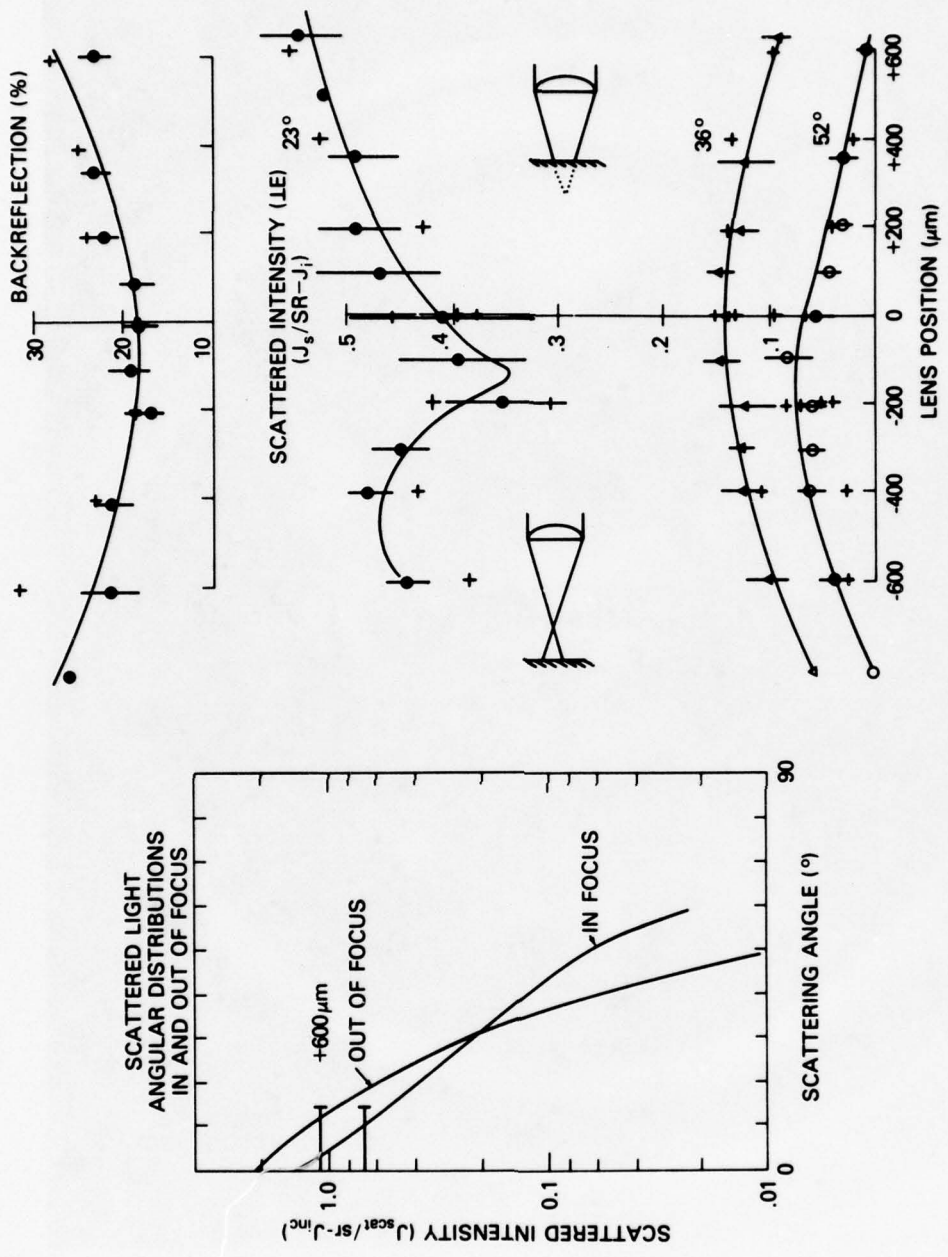


Fig. 4 - Scattered light versus focal position. Left, scattered light angular distributions in-focus and 600 μm out-of-focus. Right, scattered light intensities in the direct backscatter direction and at angles 23°, 36° and 52° to the focusing lens.

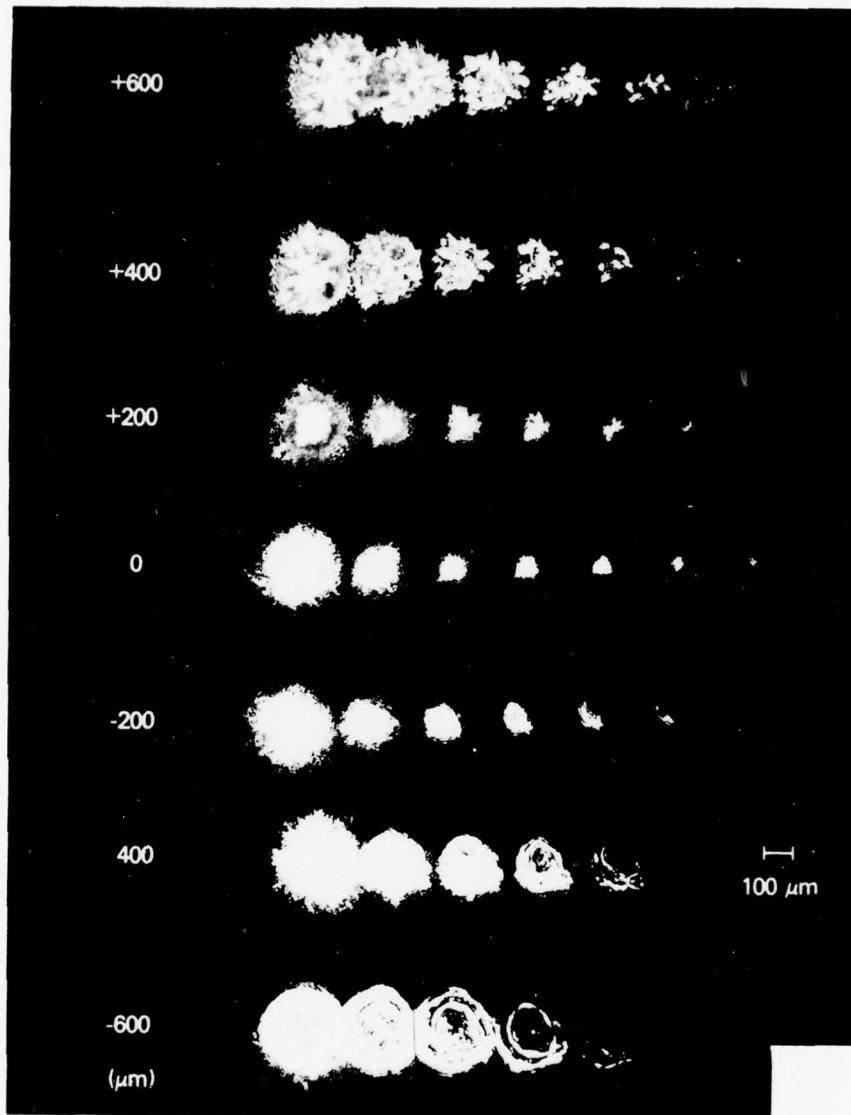


Fig. 5 - Focal spot iso-intensity distributions at the target surface for the indicated lens locations. Each contour is separated from its neighbor by 3X intensity.

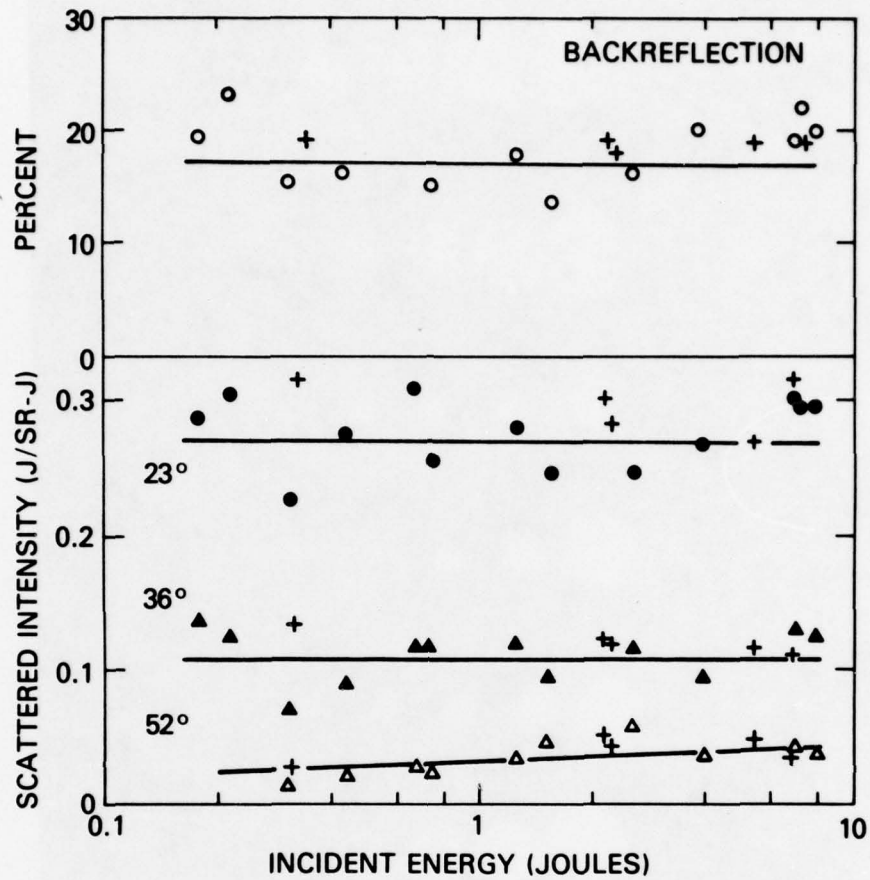
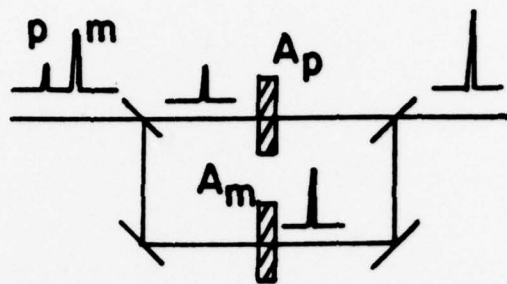


Fig. 6 - Scattered light intensities versus incident energy (irradiance) for fixed focal and beam characteristics

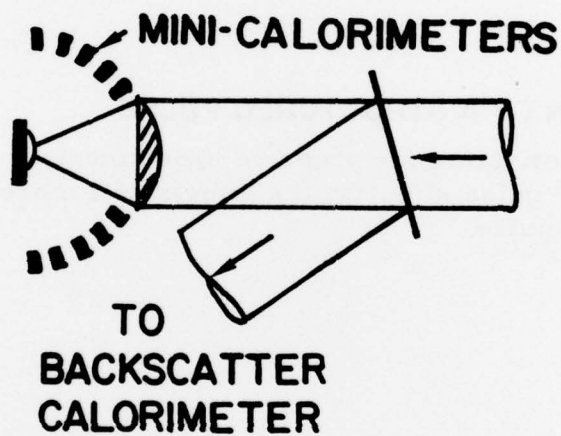


• **SIMULATION OF A STRUCTURED PULSE**

Fig. 7 - Motivation for prepulse experiments. A prepulse and "main" pulse simulate the effects of a more realistic structured pulse



(a)



(b)

Fig. 8 - (a) Beam splitting arrangement to introduce a well controlled prepulse, and (b) the experimental arrangement of scattered light calorimeters

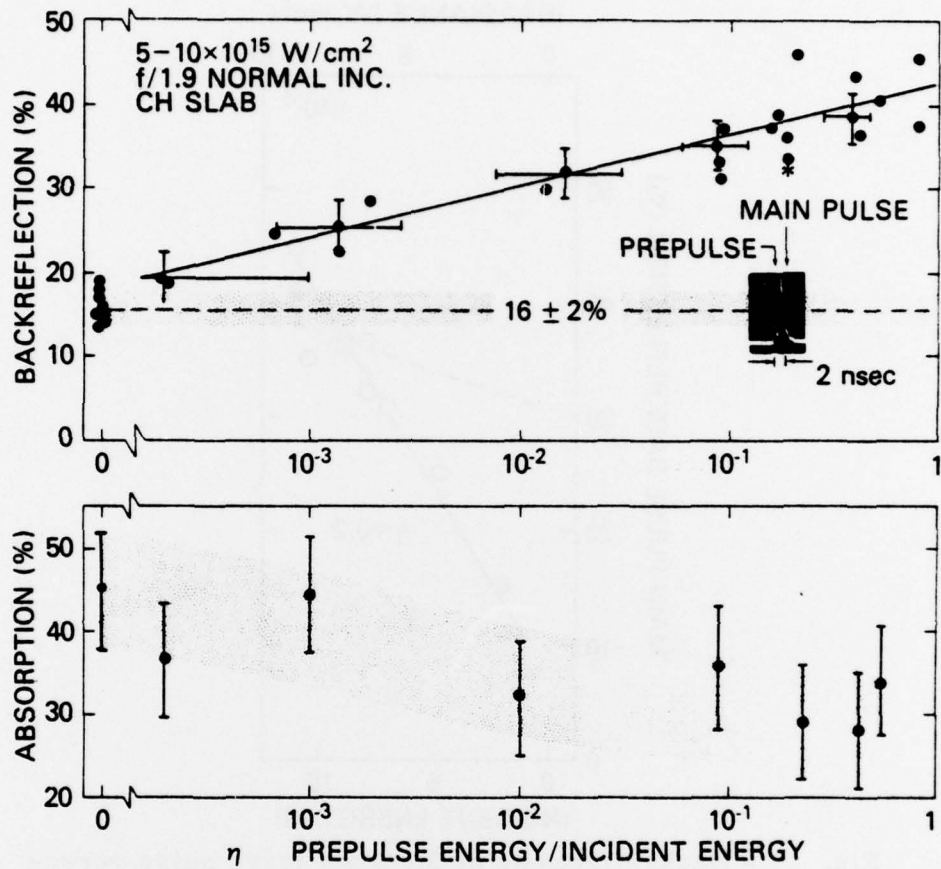


Fig. 9 - (a) Backward reflections of the main pulse versus prepulse level showing enhanced backscatter for $\eta \geq 10^{-4}$. Hashed region is the single-pulse backreflection. (b) Total absorption versus prepulse level showing a decrease in absorption with increasing prepulse level.

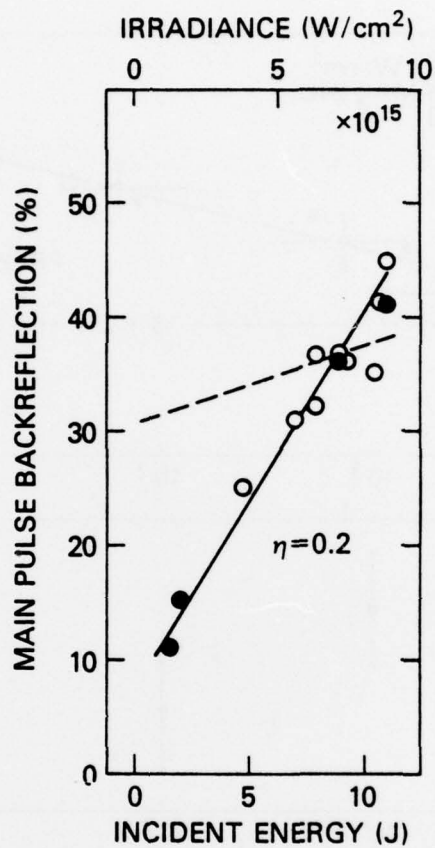


Fig. 10 - Backreflections of the main laser pulse versus the incident energy (irradiance) for a 20% prepulse [(o) $\theta = 0^\circ$, (\bullet) $\theta = 45^\circ$]. Dashed line is the decrease in the back-reflection expected due to the prepulse level dependence shown in Fig. 9a.

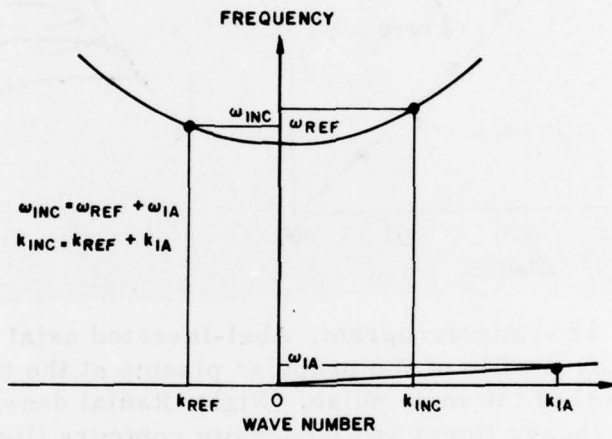
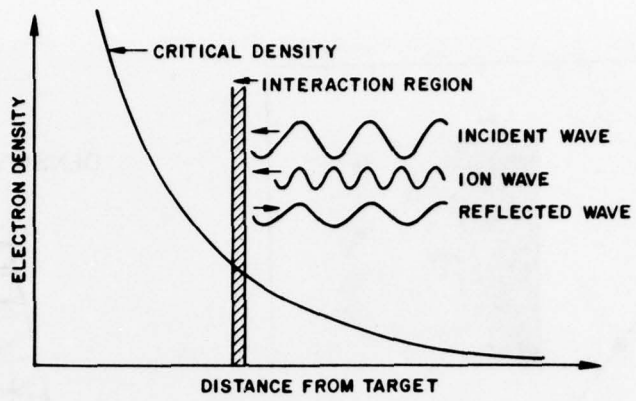


Fig. 11 - Physical model for Brillouin backscatter instability

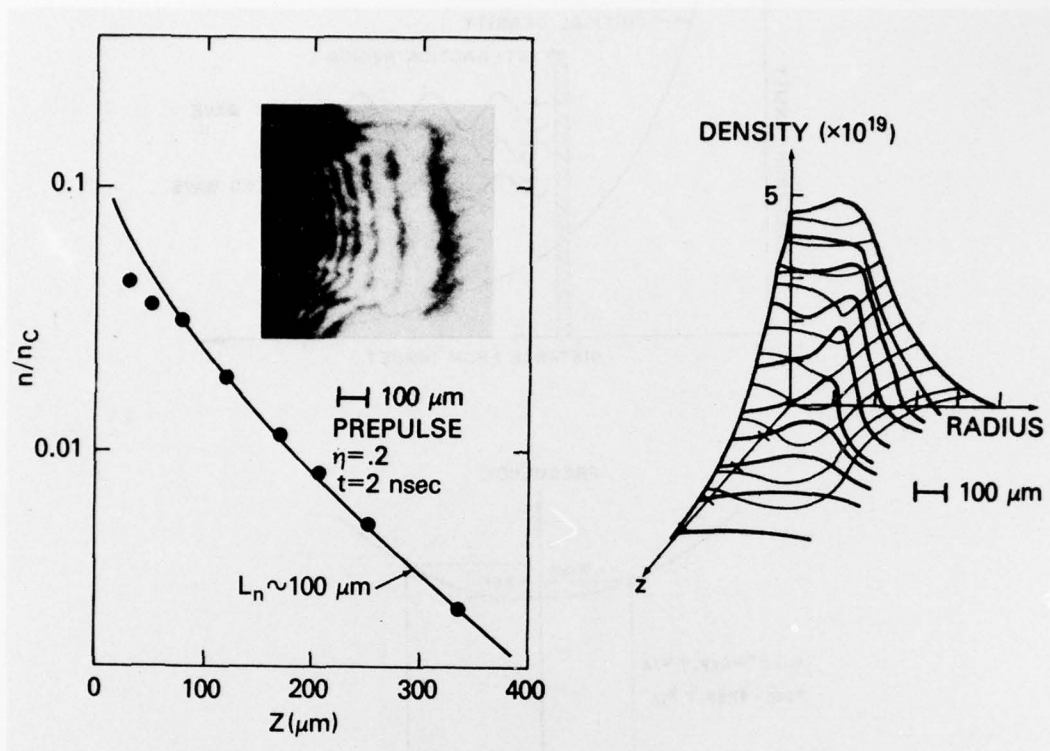


Fig. 12 - Interferogram, Abel-inverted axial electron density profile of the prepulse plasma at the time of arrival of the main pulse. Right: Radial density profiles (heavy lines) and isodensity contours (light lines) obtained from the above interferogram.

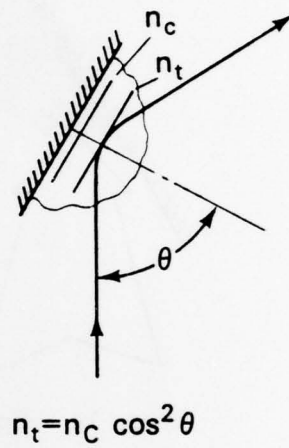
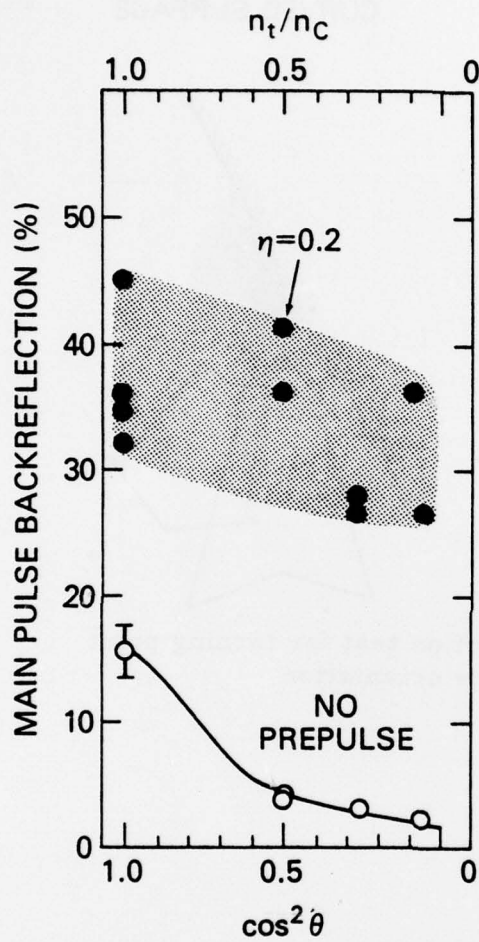


Fig. 13 - Main pulse backreflection versus target angle (θ) (or turning point density/critical density, n_t/n_c)

PLANAR SURFACE

CURVED SURFACE

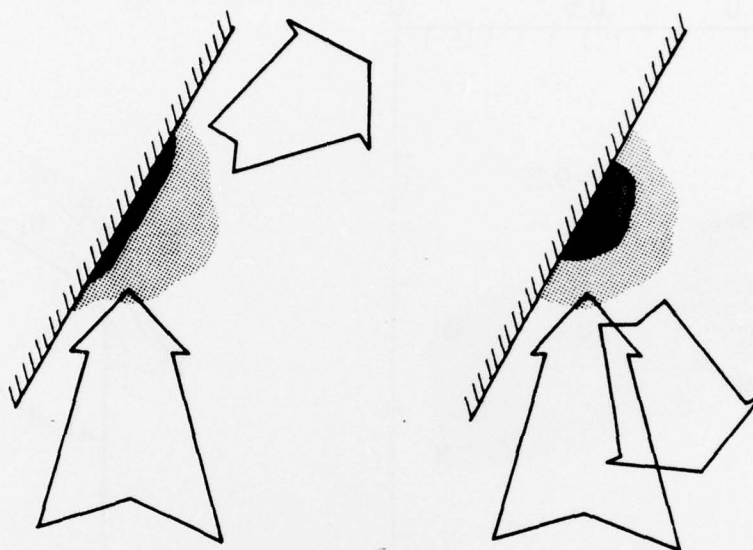


Fig. 14 - Specular reflection test for turning point density surface orientation

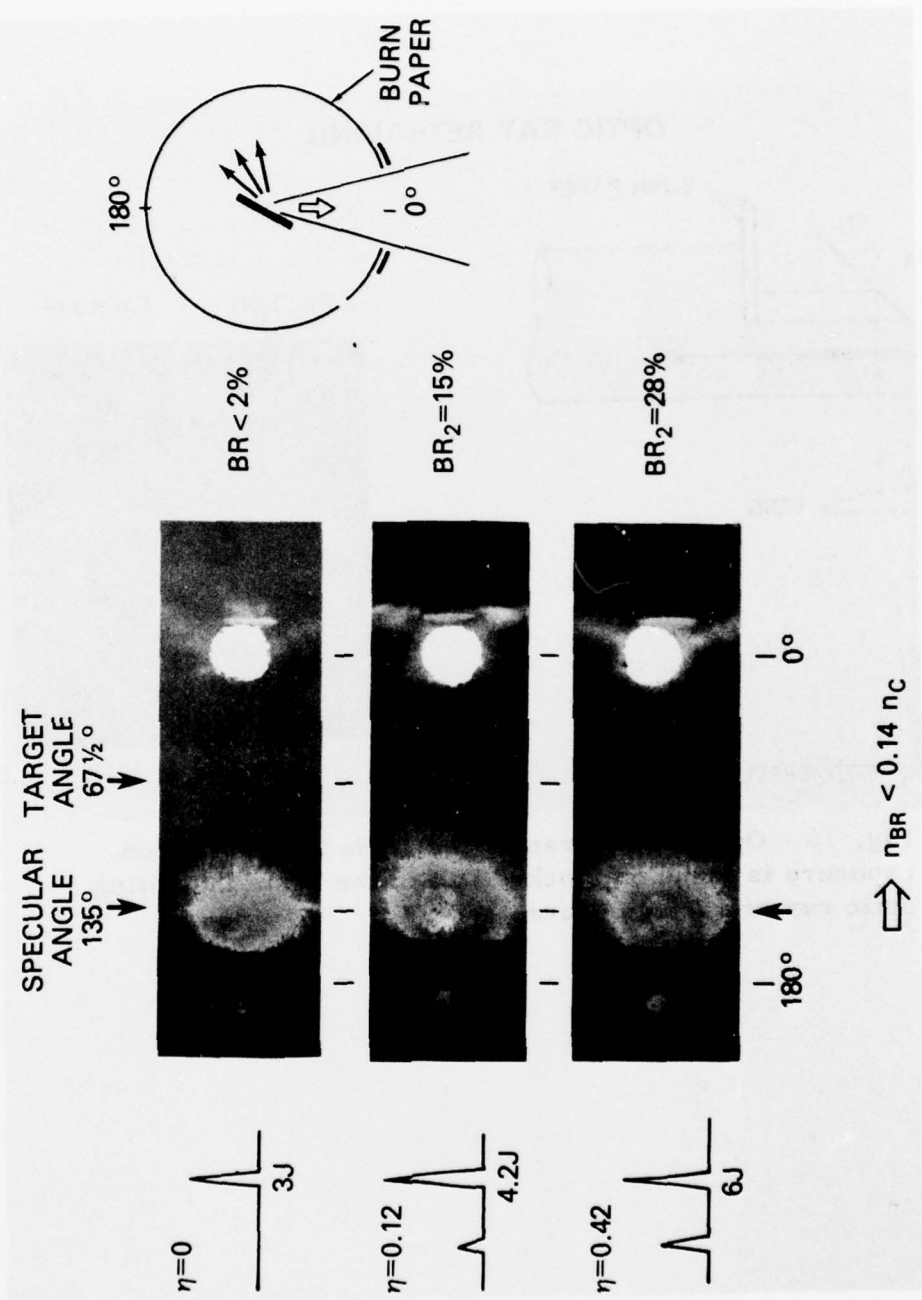


Fig. 15 - Results of specular reflection tests for turning point density surface alignment. Specular reflection occurs at target mirror angle for a single-pulse (left top), and for small and medium amplitude prepulse cases (left middle and bottom).

OPTIC RAY RETRACING

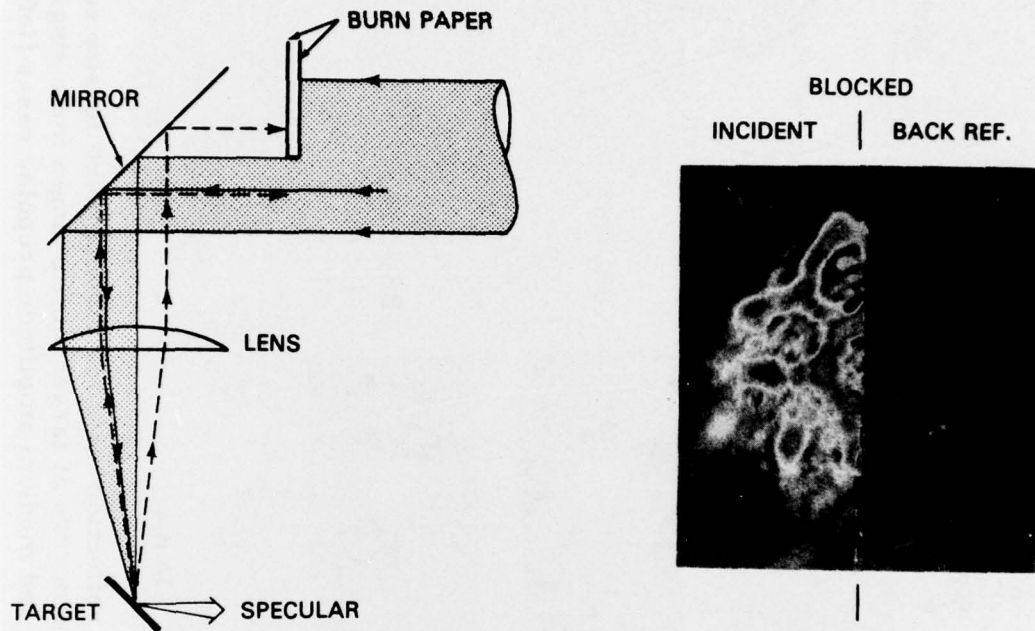


Fig. 16 - Optic ray retracing test. No backreflection exposure is found on blocked half of the beam indicating optic ray retracing occurs

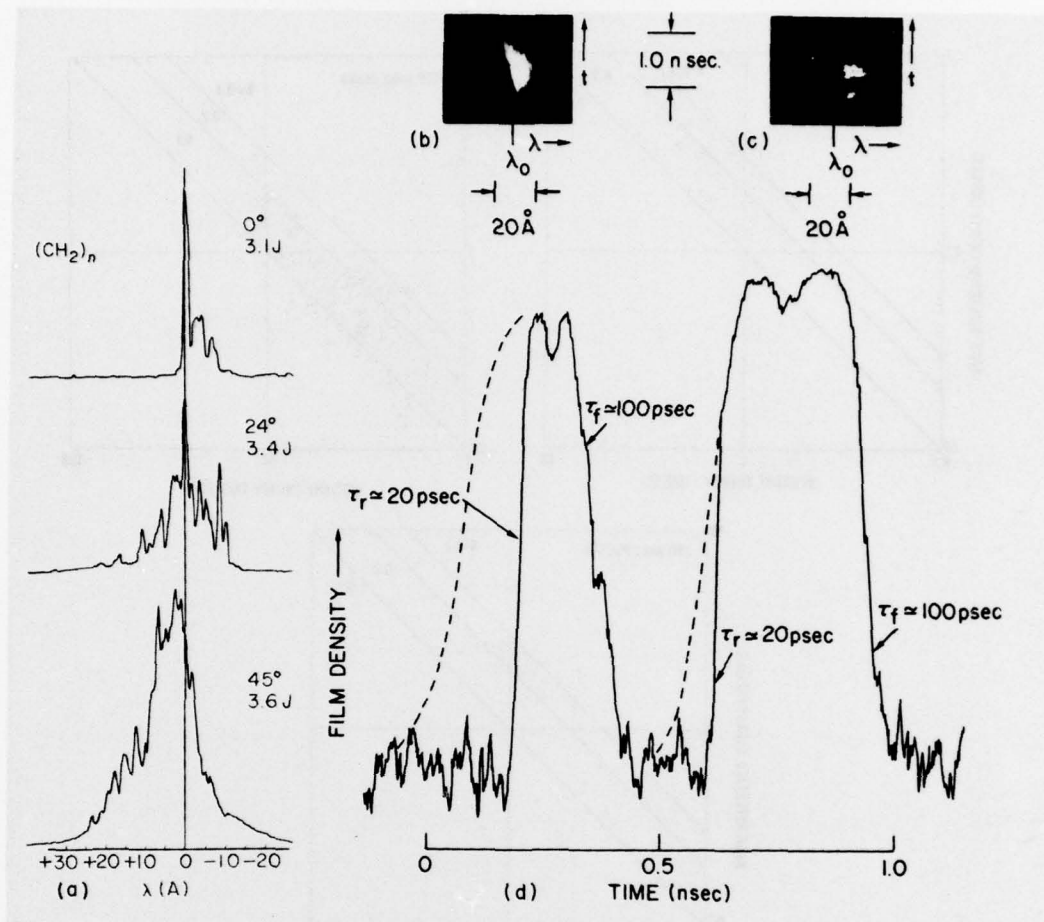


Fig. 17 - (a) Shift of backscatter time-integrated spectra towards the red for an increasing target angle θ between the target normal and the laser direction. Time-resolved backscatter spectra for (b) a copper target, f/14 lens, 8.6 J, 900 psec laser pulse with 100 psec temporal resolution, and (c) a deuterated polyethylene target f/14 lens, 16 J, 250 psec laser pulse with 20 psec temporal resolution. (d) Densitometer tracing of (c) along the time axis through the center of the spectrum. Traces have not been corrected for film exposure and are saturated at the peaks.

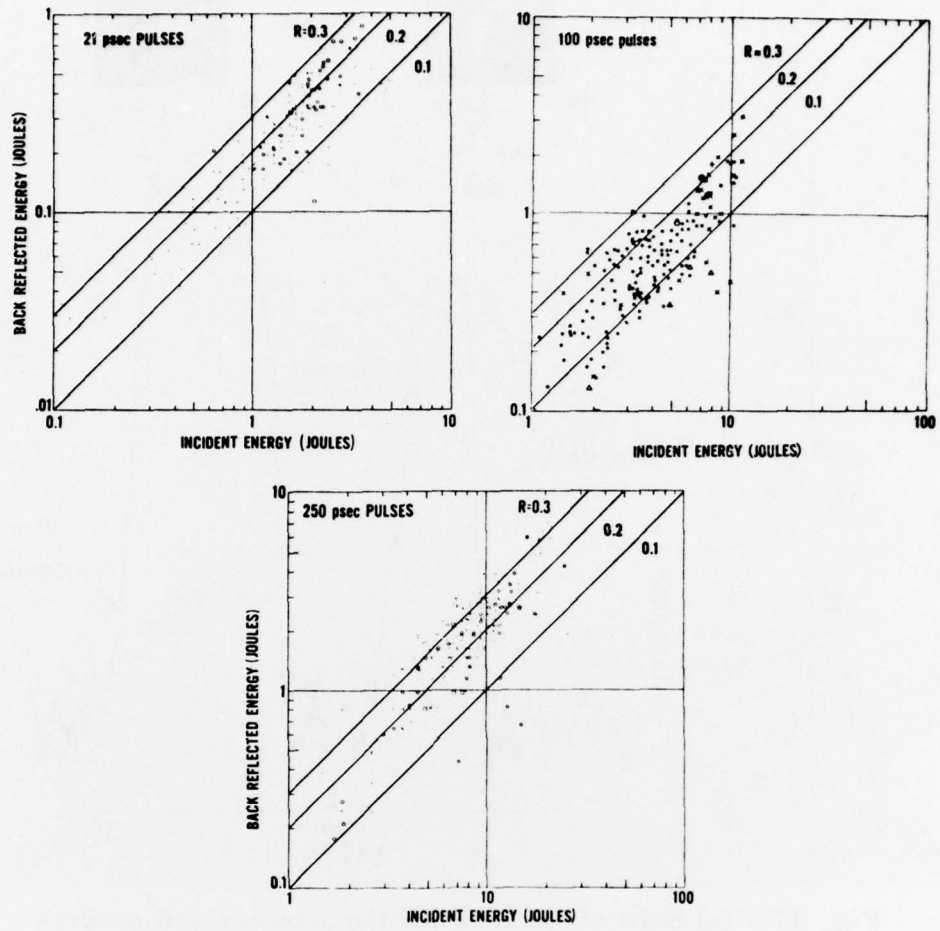


Fig. 18 - Backreflected energy versus incident energy for 21 psec pulses, 100 psec pulses and 250 psec pulses with an $f/1.9$ lens and various target materials

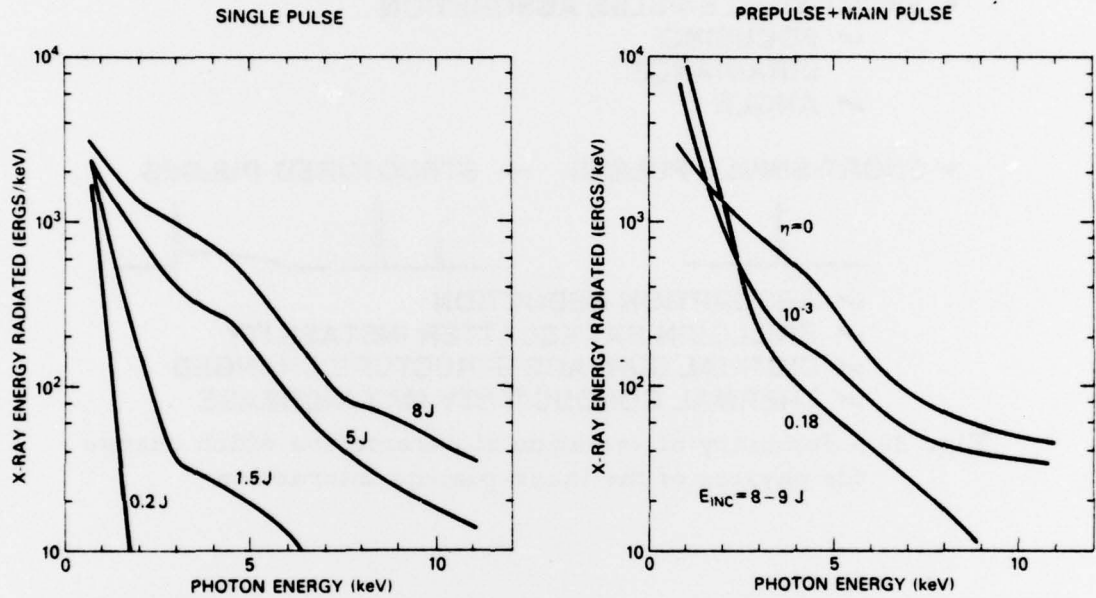


Fig. 19 - X-ray continuum spectra for single-pulse (75 psec) irradiation (left) and structured pulse irradiation (right). Note the difference in behavior near 1 keV and at higher energies for the two sets of data. This may imply a higher thermal conductivity for the structured pulse case.

- **SHORT-SINGLE-PULSE ABSORPTION**

- ✓ **FOCUSING**
- ✓ **IRRADIANCE**
- ✓ **ANGLE**

- **SHORT-SINGLE-PULSES → STRUCTURED PULSES**



- ✓ **ABSORPTION REDUCTION**
- ✓ **BRILLOUIN BACKSCATTER INSTABILITY**
- ✓ **CRITICAL SURFACE STRUCTURE CHANGED**
- ✓ **THERMAL CONDUCTIVITY MAY INCREASE**

Fig. 20 - Summary of variation of parameters which change the physics of the laser-plasma interaction